Di-hadron azimuthal correlation and Mach-like cone structure in a parton/hadron transport model

G. L. Ma[a,b], S. Zhang[a,b], Y. G. Ma[a] , H. Z. Huang[c], X. Z. Cai[a],
J. H. Chen[a,b], Z. J. He[a], J. L. Long[a], W. Q. Shen[a], X. H. Shi[a,b], J. X. Zuo[a,b]

[a] *Shanghai Institute of Applied Physics, Chinese Academy of Sciences, Shanghai 201800, China*
[b] *Graduate School of the Chinese Academy of Sciences, Beijing 100080, China*
[c] *University of California, Los Angeles,CA90095, USA*

Abstract

In the framework of a multi-phase transport model (AMPT) with both partonic and hadronic interactions, azimuthal correlations between trigger particles and associated scattering particles have been studied by the mixing-event technique. The momentum ranges of these particles are $3 < p_T^{trig} < 6$ GeV/c and $0.15 < p_T^{assoc} < 3$ GeV/c (soft), or $2.5 < p_T^{trig} < 4$ GeV/c and $1 < p_T^{assoc} < 2.5$ GeV/c (hard) in Au + Au collisions at $\sqrt{s_{NN}} = 200$ GeV. A Mach-like structure has been observed in correlation functions for central collisions. By comparing scenarios with and without parton cascade and hadronic rescattering, we show that both partonic and hadronic dynamical mechanisms contribute to the Mach-like structure of the associated particle azimuthal correlations. The contribution of hadronic dynamical process can not be ignored in the emergence of Mach-like correlations of the soft scattered associated hadrons. However, hadronic rescattering alone cannot reproduce experimental amplitude of Mach-like cone on away-side, and the parton cascade process is essential to describe experimental amplitude of Mach-like cone on away-side. In addition, both the associated multiplicity and the sum of p_T decrease, whileas the $\langle p_T \rangle$ increases, with the impact parameter in the AMPT model including partonic dynamics from string melting scenario.

Key words: di-hadron azimuthal correlation, Mach cone, parton cascade, hadronic rescattering, AMPT
PACS: 25.75.-q, 24.10.Nz, 24.10.Pa, 25.75.Ld

I. Introduction

A phase transition between hadronic matter and the quark-gluon plasma (QGP) at a critical energy density of ~ 1 GeV/fm^3 has been predicted by Quantum Chromodynamics (QCD) [1], which has motivated the scientific program at the Relativistic Heavy-Ion Collider (RHIC) at the Brookhaven National Laboratory. A very dense partonic matter has been shown to be produced in the early stage of central Au+Au collisions at $\sqrt{s_{NN}} = 200$ GeV [2]. Many interesting phenomena have been observed including the measurements of elliptic flow [3], strangeness [4], J/ψ [5] and jet quenching [6].

Email address: ygma@sinap.ac.cn.
Corresponding author (Y. G. Ma[a]).

Jet has been proved as a particularly good probe in RHIC experiments [6]. The high transverse momentum (p_T) partons (jets) which emerge from hard scattering processes will lose energy when they pass through the dense QCD medium. The energy loss (jet quenching) mechanism results in distinct experimental observations such as the disappearance of one jet in back-to-back jet correlation at high p_T [7]. At the same time, the loss energy must be redistributed in the soft p_T region [8,9,10,11]. Experimentally the soft scattered particles which carry the lost energy have been observed statistically via two-particle angular correlation of charged particles [12]. Reconstruction of these particles will constrain models which describe production mechanisms of high p_T particles, and may shed light on the underlying energy loss mechanisms and the degree of equilibration of jet products from energy loss in the medium.

A Mach-like structure (the splitting of the away side peak in di-jet correlation) has recently been observed in azimuthal correlations of scattered secondaries associated with the high p_T hadrons in central Au+Au collisions at $\sqrt{s_{NN}}$ = 200 GeV [13,14,15]. Several theoretical interpretations have been proposed for this phenomenon. For instances, Stöcker proposed Mach cone structure from jets traversing the dense medium as a probe of the equation of state and the speed of sound of the medium [16]. Casalderrey-Solana, Shuryak and Teaney argued for a shock wave generation because jets travel faster than the sound in the medium [17]. They fit the broad structure on the away side of the azimuthal correlation with a Mach cone (shock wave) mechanism; Koch and Wang et al. could produce a Mach-like structure with a Cherenkov radiation model [18]; Armesto et al. interpreted the sideward peaks as a result of medium dragging effect in Ref. [19]; Ruppert and Müller argued that the Mach-like structure can appear due to the excitation of collective plasmon waves by the moving color charge associated with the leading jet [20]; Renk and Ruppert applied a realistic model for the medium evolution to explain the observed splitting of the away side peak in Ref. [21]; Chaudhuri studied the effect on Mach-like structure from jet quenching on the hydrodynamical evolution of a QGP fluid [22]; Satarov, Stöcker and Mishustin investigated Mach shocks induced by partonic jets in expanding quark-gluon plasma [23]; A conical flow induced by heavy-quark jets was also proposed by Antinori and Shuryak [24]; Hwa et al. discussed the centrality dependence of associated particle distribution for Au + Au and d + Au, respectively, in recombination model [25]. The dynamical nature of the Mach-like structure continues to be a subject of many theoretical and experimental investigations.

There is no quantitative interpretation from dynamical transport models yet for the Mach-like structure in particle correlations from hard scattering particles interacting with the dense medium. In this work, we report a study of associated particle correlations with a triggered particle and investigate the Mach-like structure using A Multi-Phase Transport model(AMPT) [26]. We have applied the mixing-event technique in the AMPT analysis as what has been used in the analysis of RHIC collision data to remove background. We found that both parton cascade and hadronic rescattering can produce apparent correlations between triggered and associated particles similar to the Mach-like structure. But the hadronic rescattering mechanism alone is not able to produce a large enough amplitude for Mach-like cone on away side, and the parton cascade process is indispensable.

The paper is organized as follows. In Section II, we give a brief description of the AMPT model and the initial conditions. Section III describes mixing-event technique in our simulation analysis. Results and discussions are presented in Section IV. Finally a summary is given in Section V.

II. Brief description of AMPT Model

The AMPT model [26] is a hybrid model

2

which consists of four main components: the initial conditions, partonic interactions, the conversion from partonic matter into hadronic matter and hadronic rescattering interactions. The initial conditions, which include the spatial and momentum distributions of minijet partons and soft string excitation, are obtained from the HIJING model [27]. Excitation of strings will melt the string into partons. Scatterings among partons are modelled by Zhang's parton cascade model (ZPC) [28], which includes two-body scatterings with cross sections obtained from the pQCD calculations with screening mass. In the default AMPT model [29] partons are recombined with their parent strings when they stop interacting, and the resulting strings are converted to hadrons by using the Lund string fragmentation model [30]. In the AMPT model with the option of string melting [31], a quark coalescence model is used to combine partons into hadrons. Dynamics of the subsequent hadronic matter is then described by A Relativistic Transport (ART) model [32]. Details of the AMPT model can be found in a recent review [26]. Previous studies [31] have shown that the partonic effect could not be neglected and the string melting AMPT is much more appropriate than the default AMPT version when the energy density is much higher than the critical density for the predicted phase transition [26,31,33]. In the present work, the parton interaction cross section in AMPT model with string melting is assumed to be 10mb.

III. Analysis Method

In order to compare with experimental measurements of correlations between trigger and associated hadrons, we use the mixing-event technique to subtract combinatorial background in our analysis. Two ranges of p_T window selections for the trigger and associated particles have been used: one is $3 < p_T^{trig} < 6$ GeV/c and $0.15 < p_T^{assoc} < 3$ GeV/c (we call this selection as "soft" associated hadrons since soft particles dominate in this p_T range for associated particles); the other is $2.5 < p_T^{trig} < 4$ GeV/c and
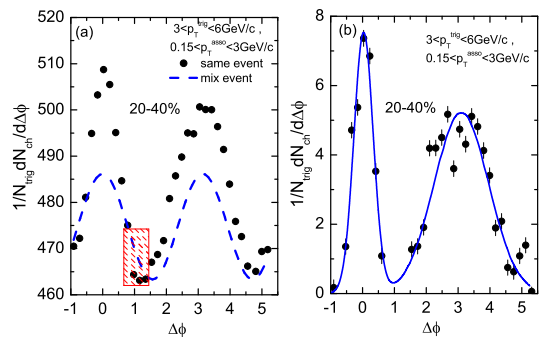

Fig. 1. (a): The $\Delta\phi$ distribution between a triggered hadron ($3 < p_T^{trig} < 6$ GeV/c) and associated hadrons ($0.15 < p_T^{assoc} < 3$ GeV/c) (circles), where the background (dash line) has not been subtracted. The data are 200 GeV Au + Au collisions with 20-40% collision centrality from the AMPT model. The dash area is the region of ZYAM normalization (see texts for detail); (b): The $\Delta\phi$ distribution where the background has been subtracted by a mixing-event technique, where the solid line is a two-Gaussian fit.

$1.0 < p_T^{assoc} < 2.5$ GeV/c (denoted as "hard" associated hadrons since there are more hard particle components than that in the "soft" selection). The triggered particles and associated particles ("soft" and "hard" ones) both are selected with a pseudo-rapidity window $|\eta| < 1.0$. In the same events, pairs of associated particles with a triggered particle are accumulated to obtain $\Delta\phi = \phi - \phi_{trig}$ distributions. In order to construct the background which is mainly from the effect of elliptic flow [12,14], a mixing-event method is applied to simulate the background. In this method, we mixed two events which have very close centrality into a new event, and extracted $\Delta\phi$ distribution to be used as background distribution. When subtracting the background from the same events, ZYAM (zero yield at minimum) assumption is adopted which has been used in the experimental analysis [14]. Figure 1 shows the $\Delta\phi$ distribution for trigger hadrons of $3 < p_T^{trig} < 6$ GeV/c and associated hadrons of $0.15 < p_T^{assoc} < 3$ GeV/c before and after the background subtraction. The data are from AMPT model simulation of Au + Au collisions at $\sqrt{s_{NN}} = 200$ GeV
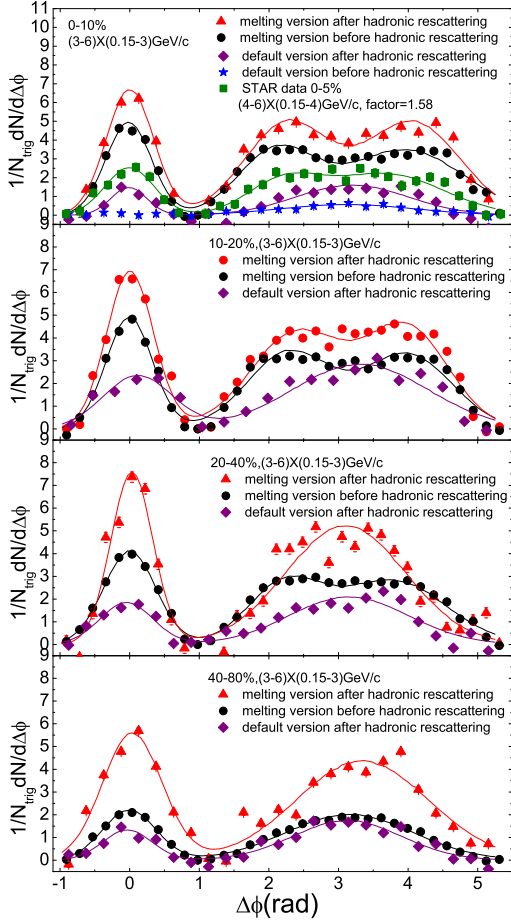
Fig. 2. Soft scattered associated hadron $\Delta\phi$ correlations for trigger hadrons of $3.0 < p_T^{trig} < 6.0 \text{GeV}/c$ and associated hadrons of $0.15 < p_T^{assoc} < 3.0 \text{ GeV}/c$ from AMPT Monte Carlo simulations of Au + Au collisions at $\sqrt{s_{NN}} = 200$ GeV with various collision centralities. Triangles: string melting version after hadronic rescattering; circles: string melting version before hadronic rescattering; diamonds: default version after hadronic rescattering; stars: default version before hadronic rescattering; squares: experimental data are from Ref [12] where $4.0 < p_T^{trig} < 6.0 \text{ GeV}/c$ and $0.15 < p_T^{assoc} < 4.0 \text{ GeV}/c$.

for 20-40% collision centrality, where the string melting mechanism has been turned on.

IV. Results and Discussions

In Ref. [12], it was found that the $\Delta\phi = \phi - \phi_{trig}$ distribution of recoiling hadrons from a high p_T triggered particle is significantly broadened in central Au + Au collisions at $\sqrt{s_{NN}} = 200$ GeV, which supports the picture of the dissipation of jet energy in the medium. In order to increase the statistical sample of triggered particles in our calculation, we set p_T range for trigger particles to $3 < p_T^{trig} < 6 \text{ GeV}/c$ and for associated particles to $0.15 < p_T^{assoc} < 3 \text{ GeV}/c$ in our analysis. Both triggered and associated particles are further selected with a pseudo-rapidity cut of $|\eta| < 1.0$.

Figure 2 presents AMPT model calculations of soft associated hadron $\Delta\phi$ correlations from Au + Au collisions at $\sqrt{s_{NN}} = 200$ GeV for different centralities under various AMPT running conditions. In order to compare our results with experimental data which give the correlations among associated charged hadrons, the experimental data are multiplied by a factor of 1.58 to account for the contribution from neutral hadrons [12,35]. Note that for the default AMPT version before hadronic rescattering, we here give $\Delta\phi$ correlation for 0-10% collision centrality only due to the lack of statistics obtained for other centrality bins. We found that the hadronic rescattering increases $\Delta\phi$ correlation yields for both versions. A very strong Mach-like structure is observed for central Au+Au collisions before hadronic rescattering in the melting AMPT version, which indicates that the Mach-like structure has been formed in parton cascade process. The effect of hadronic rescattering on the $\Delta\phi$ correlation in central collisions ($< 20\%$ centrality) does not wash out, even slightly enhances, the Mach-like structure, which is qualitatively in agreement with the effect of time-dependent speed of sound on the development of the conical wave in expanding QCD matter [36].

Figure 3 shows the AMPT calculations of $\Delta\phi$ correlations between a triggered particle of $2.5 < p_T^{trig} < 4.0 \text{GeV}/c$ and hard associated particles of $1.0 < p_T^{assoc} < 2.5$ GeV/c from Au + Au collisions at $\sqrt{s_{NN}} = 200$ GeV for various centralities, where
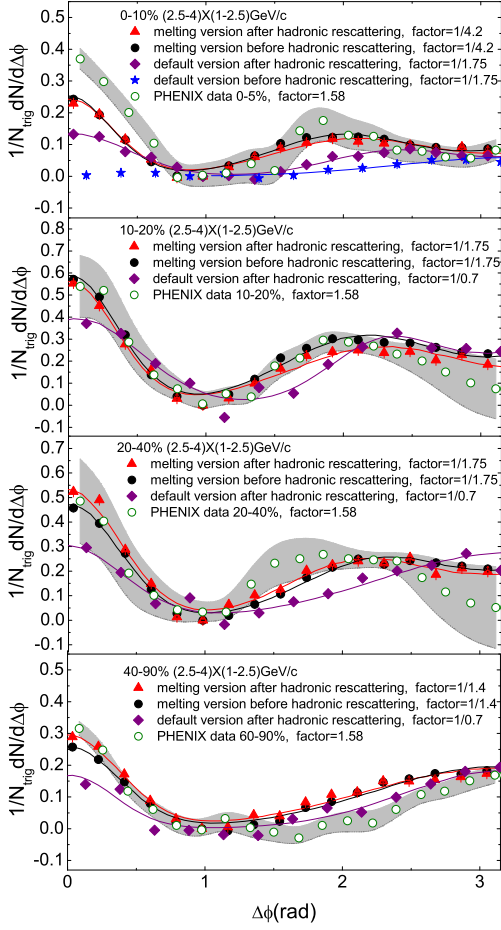
4

Fig. 3. AMPT model calculations of $\Delta\phi$ correlations between a triggered hadron of $2.5 < p_T^{trig} < 4.0$ GeV/c and hard associated hadrons of $1.0 < p_T^{assoc} < 2.5$ GeV/c from Au + Au collisions at $\sqrt{s_{NN}} = 200$ GeV in various centralities. Triangles: AMPT version with string melting after hadronic rescattering; Full circles: AMPT version with string melting before hadronic rescattering; Diamonds: default AMPT version after hadronic rescattering; Stars: default AMPT version before hadronic rescattering; Open circles: experimental data from Ref. [14]; Hatched areas indicate the experimental uncertainty. Note that the scaling factors may also reflect different pseudorapidity ranges used in experimental data analysis and model calculations. See text for details.

pseudorapidity cuts of $|\eta^{trig}| < 1.0$ and $|\eta^{assoc}| < 1.0$) have also been applied. We found that the effect on $\Delta\phi$ correlations from hadronic rescattering is much smaller than the case for soft associated particles,

which may indicate that fewer fraction of hard associated hadrons suffer hadronic rescattering. In addition, Mach-like structures have been observed on away-side correlations in both string-melting and default AMPT versions. In the default AMPT version, however, the Mach-like structures can be observed only after turning on hadronic rescatterings.

The default AMPT version appears to produce the number of associated particles matching better with the experimental measurement than that from the string-melting AMPT version. This may be attributed to the fact that the string-melting AMPT model always produces softer p_T spectra than the default AMPT model because current quark masses have been used in the partonic cascade stage [26]. It may be improved if thermal parton masses are applied [34]. However, in the present study, we only focus on the correlation shape instead of yields in the correlation region. In this context, we shall compare the shapes of $\Delta\phi$ correlation functions between the AMPT model and experimental data. To this end, the AMPT model data have been multiplied with different normalization factors which are listed on right sides of each panel in Figure 3. Please note that there is a difference for pseudo-rapidity cut between our simulation and the experimental data. Our simulation cut of associated particle is $|\eta| < 1.0$ (due to the limited statistics),while $|\eta| < 0.35$ in PHENIX data. In this case, the scaling factors of our simulation should be reduced by a factor of about 3 in order to match the data. By this reduction, the scaling parameters shown in the figures have been normalized to the same $|\eta|$ cuts as the data. However, even with the scaling of 3 these factors still deviate from 1 and show a centrality dependence. These deviations can be attributed to the following facts: (1) a large yield of particles in the correlation region can partially come from the fact that our p_T spectra in AMPT calculation with string melting scenario is under-predicted in high p_T region if we compare with the experimental data. In this case, the soft component will be over-predicted if we compare $\frac{dN}{N_{trig}d\Delta\phi}$ between
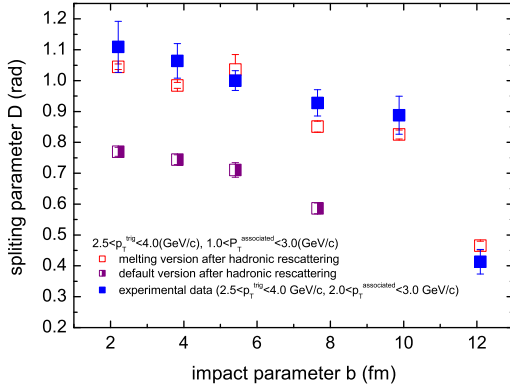
Fig. 4. Splitting parameter D versus impact parameter for Au + Au collisions at $\sqrt{s_{NN}}$ = 200 GeV (p_T windows in model: $2.5 < p_T^{trig} < 4.0$ GeV/c and $1.0 < p_T^{assoc} < 3$ GeV/c; p_T windows in experiments: $2.5 < p_T^{trig} < 4$ GeV/c and $2.0 < p_T^{assoc} < 3.0$ GeV/c). Open symbols: the string-melting version with hadron rescatterings; half filled symbols: the default version with hadronic rescatterings; filled symbols: experimental data from Ref. [15].

the data and simulation; (2) the centrality dependence of scaling factors may stem from more excessive parton interactions when a jet parton passes through various dense partonic matter depending on the collision centrality. In this study, our emphasis will be on the comparison of shapes of the Mach-like structure between the AMTP model calculations and experimental data. Our simulation results indicate that the string-melting AMPT model can describe shapes of $\Delta\phi$ correlations between a triggered hadron and associated particles better than the default AMPT model, especially for central Au+Au collisions.

In order to quantitatively characterize the Mach-like structure, a splitting parameter D has been extracted in our analysis. The splitting parameter D is defined as half distance between two Gaussian peaks on away side of associated particle $\Delta\phi$ correlations. The D value reflects the size of direction-splitting of Mach-cone on the away side. Figure 4 shows the impact parameter dependence of D. Our results in-

dicate that the string-melting AMPT version can roughly match the experimental data. Note that of our p_T cuts are slightly different from experimental cuts in order to increase our statistics. However, D values from the default AMPT version are significantly smaller than the experimental data. We conclude that hadronic rescattering mechanism alone is not enough to produce the amplitude of Mach-like cone structure on the away side and parton cascade mechanism is necessary. It should be noted that minijet partons produced from hard scatterings can lose energy by gluon radiations and transfer their energies to nearby soft strings in the HIJING model, which has been called jet quenching [27]. In the AMPT model, the jet quenching in the HIJING model is replaced by parton scatterings from the ZPC. Only two-body scatterings are included in the current ZPC, and higher-order contributions such as $2 \rightleftharpoons 3$ scattering processes to the jet energy loss are still missing in our AMPT calculations. It has been proposed that higher order processes may contribute significantly to the observed large jet quenching [37]. However our results indicate that $2 \rightleftharpoons 2$ processes could account for most of the amplitude for the Mach-like structure. The AMPT version with string melting scenario has also been shown to generate elliptic flow of hadrons better than the default version. Furthermore, it can reproduce the mass ordering in the particle dependence of elliptic flow, which can be described by hydrodynamics models [31,33]. It is believed that the big cross section for parton interactions used in the AMPT model leads to strong parton cascades that couple partons together, resulting the onset of hydrodynamics behavior from parton cascades [38]. It has also been proposed that a Mach-like structure can be generated if the jet velocity is faster than the sound velocity when the jet traverses through the dense matter [16,17]. In addition, continuous partonic rescatterings and the rapid expansion of the dense medium can also lead to parton's direction in the medium to both sides of triggered particle direction, which may result in an apparent Mach-like structure in the AMPT model. Nevertheless, we conclude that sig-

6

nificant parton cascades are essential in order to describe elliptic flow of hadrons and the Mach-like structure in particle $\Delta\phi$ correlations simultaneously.

We have also investigated several characteristics of soft associated particles in the AMPT model with the string-melting scenario. Figure 5 shows a comparison between experimental data and our AMPT calculation results with hadronic rescatterings. Panel (a) in Fig. 5 shows the number of associated hadrons as a function of impact parameter in Au+Au collisions at $\sqrt{s_{NN}} = 200$ GeV. The trigger particles are not included in the N_{ch} counting for the near side. The number of average associated hadrons decreases with increasing impact parameters in the model as well as in the experiment. However, the number of associated hadrons in the AMPT model is much larger than the experimental data on both near and away sides, which may due to different p_T cuts used in the model calculation and experimental data. Panel (b) shows the p_T distributions of the associated hadrons on near side and away side in most central (0-5% centrality) Au + Au collisions at $\sqrt{s_{NN}} = 200$ GeV. Panel (c) gives the sum of p_T magnitude, which approximates to associated energy, as a function of impact parameter. The triggered particles are included in the p_T magnitude sum for the near side. The sums of p_T magnitude decrease with impact parameters for both near side and away side, and theoretical values are somewhat higher than the experimental data, again may be affected by the different p_T cuts. Panel (d) displays the dependence of $\langle p_T \rangle$ on impact parameters on away side. $\langle p_T \rangle$ increases with impact parameter. These comparisons may help to address the issue of parton thermalization through the parton cascade mechanism in central Au+Au collisions [12].

V. Conclusions

In summary, the origin of the Mach-like structure in correlations between triggered hadrons and soft or hard associated particles has been investigated in the framework of a hybrid dynamics transport model
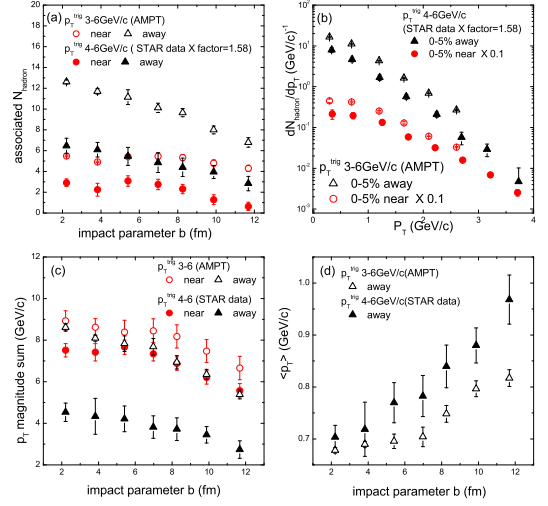

Fig. 5. Comparisons between model calculations (p_T windows: $3 < p_T^{trig} < 6$ GeV/c and $0.15 < p_T^{assoc} < 3$ GeV/c) and experimental data [12] (p_T windows: $4 < p_T^{trig} < 6$ GeV/c and $0.15 < p_T^{assoc} < 4$ GeV/c) in Au + Au collisions at $\sqrt{s_{NN}} = 200$ GeV. Open symbols: calculations from the string-melting AMPT version, filled symbols: experimental data, circle: near side, triangle: away side. Panel (a): Number of associated hadrons versus impact parameter; Panel (b): p_T distributions for the associated hadrons on near side and away side for 0-5% centrality; Panel (c): Sum of p_T magnitude as a function of impact parameter on near side and away side; Panel (d): $\langle p_T \rangle$ as a function of impact parameter on away side.

which includes two dynamical processes, namely parton cascade and hadronic rescattering. By comparing the different calculation results with or without parton cascade, before or after hadronic rescattering, we found that the associated particle correlations and the Mach-like structure have been formed mostly before hadronic rescatterings, which indicates that these kinds of correlations are born in the partonic process and are further developed in the later hadronic rescattering processes. For the hard associated particles, hadronic rescattering hardly changes the Mach-like structure which is mostly formed in parton cascade processes. Therefore, characteristics of hard associated particles may directly reflect information of intrinsic par-

tonic dynamics. Meanwhile, the effect of hadronic rescattering can not be ignored especially for soft associated particles, because many of these soft associated particles either are produced in or suffer from hadronic rescattering processes. Our calculations indicate that hadronic rescattering mechanism alone is unable to produce a splitting parameters D distribution for the Mach-like structure matching the experimental data. The parton cascade mechanism is essential for the Mach-like structure while the exact shape and strength of the azimuthal correlations seem to depend on detailed properties of the partonic medium and jet, which still awaits quantitative explanations.

Acknowledgements

References

[1] F. Karsch, Nucl. Phys. **A698**, 199c (2002).

[2] I. Arsene et al., Nucl. Phys. A **757**, 1 (2005); B. B. Back et al., Nucl. Phys. A **757**, 28 (2005); J. Adams et al., Nucl. Phys. A **757**, 102 (2005); S. S. Adler et al. (PHENIX Collaboration), Nucl. Phys. A **757**, 184 (2005).

[3] J. Adams et al. (STAR Collaboration), Phys. Rev. Lett. **95**, 122301 (2005); J. Adams et al. (STAR Collaboration), Phys. Rev. Lett. **93**, 252301 (2004).

[4] J. Adams et al. (STAR Collaboration), Phys. Lett. B **612**, 181 (2005).

[5] S.S. Adler et al. [PHENIX Collaboration], Phys. Rev. Lett. **96**, 012304 (2006).

[6] C. Adler et al. (STAR Collaboration), Phys. Rev. Lett. **91**, 072304 (2003) ; J. Adams et al (STAR Collaboration), Phys. Rev. C **73**, 064907 (2006); J. Adams et al (STAR Collaboration), arXiv: nucl-ex/0408012 ; S. S. Adler et al. (PHENIX Collaboration), Phys. Rev. Lett. **91**, 072301 (2003); S. S. Adler et al. (PHENIX Collaboration), Phys. Rev. C **73**, 054903 (2006); S. S. Adler et al. (PHENIX Collaboration), Phys. Rev. C **71**, 051902 (2005).

[7] C. Adler et al. (STAR Collaboration), Phys. Rev. Lett. **90**, 082302 (2003).

[8] S. Pal and S. Pratt, Phys. Lett. B **574**, 21 (2003).

[9] C. A. Salgado and U.A. Wiedemann, Phys. Rev. Lett. **93**, 042301 (2004).

[10] I. Vitev, Phys. Rev. D **71**, 054027 (2005).

[11] X.-N. Wang, Phys. Lett. B **579**, 299 (2004).

[12] J. Adams et al. (STAR Collaboration), Phys. Rev. Lett. **95**, 152301 (2005).

[13] J. G. Ulery [STAR Collaboration], Nucl. Phys. A **774**, 581 (2006).

[14] S. S. Adler et al. [PHENIX Collaboration], Phys. Rev. Lett. **97**, 052301 (2006).

[15] Jiangyong Jia [PHENIX Collaboration], arXiv:nucl-ex/0510019.

[16] H. Stöcker, Nucl. Phys. A **750**, 121 (2005).

[17] J. Casalderrey-Solana, E. V. Shuryak, D. Teaney, J. Phys. Conf. Ser. **27**, 22 (2005).

[18] V. Koch, A. Majumder, Xin-Nian Wang, Phys. Rev. Lett. **96**, 172302 (2006).

[19] N. Armesto, C. A. Salgado, Urs. A. Wiedemann, Phys. Rev. C**72**, 064910 (2005).

[20] J. Ruppert, B.Müller, Phys. Lett. B **618**, 123 (2005) .

[21] T. Renk and J. Ruppert, Phys. Rev. C **73**, 011901(R) (2006).

[22] A. K. Chaudhuri, arXiv:nucl-th/0503028.

[23] L. M. Satarov, H. Stöcker and I. N. Mishustin, Phys. Lett. B **627**, 64 (2005).

[24] F. Antinori and E. V. Shuryak, J. Phys. G **31**, L19 (2005).

[25] R. Hwa and Z. Tan, Phys. Rev. C **72**, 057902 (2005).

[26] Z. W. Lin, C. M. Ko, B. A. Li, B. Zhang, S. Pal, Phys. Rev. C **72**, 064901 (2005).

[27] X.-N. Wang and M. Gyulassy, Phys. Rev. D **44** 3501 (1991); M. Gyulassy and X.-N. Wang, Comput. Phys. Commun. **83**, 307 (1994).

[28] B. Zhang, Comput. Phys. Commun. **109** 193 (1998).

[29] B. Zhang, C. M. Ko et al., Phys. Rev. C **61**, 067901 (2000).

[30] B. Andersson, G. Gustafson et al., Phys. Rep. **97** 31 (1983).

[31] Z.W. Lin, C. M. Ko, Phys. Rev. C **65**, 034904 (2002); Z. W. Lin, C. M. Ko et al., Phys. Rev. Lett. **89**, 152301 (2002) .

[32] B. A. Li and C. M. Ko, Phys. Rev. C **52** 2037 (1995).

[33] J. H. Chen, Y. G. Ma, G. L. Ma et al., arXiv:nucl-th/0504055.

[34] C. M. Ko, Private Communication.

[35] J. Adams et al. (STAR Collaboration), Phys. Rev. Lett. **92**, 112301 (2004); S.S. Adler et al. (PHENIX Collaboration), Phys. Rev. C **69**, 034909 (2004).

[36] J. Casalderrey-Solana, E. V. Shuryak, arXiv:hep-ph/0511263.

[37] Z. Xu and C. Greiner, Phys. Rev. C **71**, 064901 (2005).

[38] Bin Zhang, Miklos Gyulassy and Che Ming Ko, Phys.Lett. B **455**, 45 (1999).